Investigation of the Correlation of Sensitivity Vectors of Hydrogen Combustion Models

JUDIT ZÁDOR, ISTVÁN GY. ZSÉLY, TAMÁS TURÁNYI

Department of Physical Chemistry, Eötvös University (ELTE), H-1518 *Budapest, Hungary*

Received 10 March 2003; accepted 21 November 2003

DOI 10.1002/kin.10193

ABSTRACT: A well-established method for the analysis of large reaction mechanisms is the calculation and interpretation of the sensitivity of the kinetic model output Y_i to parameter changes. Comparison of the sensitivity vectors $\mathbf{s}_i = \{\partial Y_i/\partial \mathbf{p}\}$ belonging to different model outputs is a new tool for kinetic analysis. The relationship of the sensitivity vectors was investigated in homogeneous explosions, freely propagating and burner-stabilized laminar flames of hydrogen–air mixtures, using either calculated adiabatic or constrained temperature profiles, for fuel-to-air ratios $\varphi = 0.5$–4.0. Sensitivity vectors are called locally similar, if the relationship $\mathbf{s}_i = \lambda_{ij}\mathbf{s}_j$ is valid, where λ_{ij} is a scalar. In many systems, only approximate local similarity of the sensitivity vectors exists and the extent of it can be quantified by using an appropriate *correlation function*. In the cases of adiabatic explosions and burner-stabilized flames, accurate local similarity was present in wide ranges of the independent variable (time or distance), and the correlation function indicated that the local similarity was not valid near the concentration extremes of the corresponding species. The regions of poor similarity were studied further by *cobweb plots*. The correlation relationships found could be interpreted by the various kinetic processes in the hydrogen combustion systems. The sensitivity vector of the laminar flame velocity is usually considered to be characteristic for the whole combustion process. Our investigations showed that the flame velocity sensitivity vector has good correlation with the H and H_2O concentration sensitivities at the front of the adiabatic flames, but there is poor correlation with the sensitivity vectors of all concentrations in homogeneous explosions. © 2004 Wiley Periodicals, Inc. Int J Chem Kinet 36: 238–252, 2004

INTRODUCTION

Sensitivity analysis is a widely used tool for the study of chemical kinetic models [1]. Most simulation programs in reaction kinetics calculate local sensitivity coefficients $s_{ik} = \{\partial Y_i/\partial p_k\}$, which show the change of model output Y_i if parameter p_k has been slightly changed. If the results of the model are time dependent, the sensitivity coefficients are also functions of time. In spatially one-dimensional stationary reaction-diffusion systems, like stationary 1-D laminar flames, the sensitivity coefficients are functions of distance.

In the case of a general mathematical model, no relation is expected among the rows and/or the columns

Correspondence to: Tamás Turányi; e-mail: turanyi@garfield.chem.elte.hu.

Contract grant sponsor: OTKA.

Contract grant number: T043770.

of the sensitivity matrix $\mathbf{S} = \{s_{ik}\}$. However, in several kinetic systems the following relationships have been observed [2,3]:

i. *Local similarity:* The value

$$\lambda_{ij}(z) = \frac{s_{ik}(z)}{s_{jk}(z)} \tag{1}$$

depends on the independent variable z (time or distance) and the selected model output Y_i and Y_j, but is independent of the perturbed parameter p_k. Consequently, if output Y_i is very sensitive to a parameter, then so is Y_j, and if output Y_i is not sensitive to a parameter, then output Y_j is also not sensitive to it. In other words, at z the relative importance of the parameters for any variable can be told by looking at the sensitivity coefficients of only one, arbitrarily selected variable.

ii. *Scaling relation:* The ratio

$$\frac{\mathrm{d}Y_i/\mathrm{d}z}{\mathrm{d}Y_j/\mathrm{d}z} = \frac{s_{ik}(z)}{s_{jk}(z)} \tag{2}$$

holds for any parameter p_k. Existence of scaling relation includes the presence of local similarity, but local similarity may exist without the scaling relation.

iii. *Global similarity:* The value

$$\mu_{km} = \frac{s_{ik}(z)}{s_{im}(z)} \tag{3}$$

is independent of z within the interval (z_1, z_2) and the model output studied.

Similarity of sensitivity functions was first detected by Reuven et al. [4]. They had created a computer code for the calculation of local sensitivities of stationary two-point boundary value problems and tested the code on a simple model of 1-D laminar flames using a small mechanism of two reactions. Smooke et al. [5] used this program for the calculation of stationary adiabatic premixed laminar hydrogen–air flames, and global similarity of the sensitivity curves was found. They called it self-similarity, although this term had been used for another notion in fractal theory. Smooke et al. [5] also detected the scaling relation. Mishra et al. [6] applied the code for the calculation of sensitivities of adiabatic premixed burner-stabilized laminar $CO/H_2/O_2$ flames and they reported both global similarity and the scaling relation. They calculated and plotted the sensitivities of the CO concentration with respect to the rate coefficients and to the diffusion coefficients of the important species, and found that these functions cross zero at the same point and that their extremes coincide. Although they did not calculate the ratios, the presented graphs show that similarity also exists at other distances. Mishra et al. [6] also carried out *constrained temperature* calculations. In this case, the temperature–distance curve was fixed in such a way that it matched exactly the calculated adiabatic temperature–distance curve, thus the calculated concentration–distance functions were identical to those of the adiabatic case. However, the parameter perturbations leave the constrained temperature profile unchanged, and it affects the concentration sensitivities, making them much smaller. Mishra et al. [6] also found that the similarity relations were not valid for the constrained temperature system. These observations indicated the importance of temperature as a variable that strongly couples the other variables in adiabatic combustion systems.

Rabitz and Smooke [3] claimed that the onset of scaling relations and global similarity could be explained by assuming that there is a single *dominant variable* in the system. According to their definition, a variable is called dominant if changing the value of it changes the values of all other variables, but perturbation of the value of a nondominant variable changes the values of other nondominant variables most significantly through the perturbation of the value of the dominant variable. They claimed that it means that the value of any dependent variable can be obtained as a function of the dominant variable only. In their paper [3], temperature was assumed to be the single dominant variable in adiabatic combustion models. Vajda et al. [7] investigated this subject by comparing sensitivity functions of models of adiabatic explosions and laminar flames of hydrogen–air mixtures. They concluded that the sensitivity functions of flames are much more similar than those of homogeneous explosions. Vajda and Rabitz [8] studied thermal explosions modelled by a single step, nth-order, exothermic reaction. Their model had two variables: temperature and fuel concentration. Global similarity was observed for parameter sets where the model simulated thermal runaway. In a dynamical system, the parameter perturbation causes a shift in the values of the system variables, which induces further changes of these values. The system of sensitivity differential equations are called *pseudohomogeneous*, if after some time (and/or distance) this indirect effect on the system variables is much more significant than the direct effect of the parameter perturbation. Vajda and Rabitz [8] stated that the onset of global similarity for explosions could be explained if the model has two properties: temperature is the single dominant variable and the sensitivity equations are pseudohomogeneous within a time window.

Zsély et al. [2] reinvestigated the similarity of sensitivities of various models of hydrogen–air combustion. They reported local similarity, scaling relation, and global similarity of sensitivity functions of adiabatic explosions. Constrained temperature explosions (using the same concept as Mishra et al. [6], discussed above) showed local similarity for a group of parameters, but scaling relation was not valid in this case. Adiabatic burner-stabilized flames showed all three types of similarity, but only for a part of the parameters. No similarity was found for freely propagating flames and for constrained temperature burner-stabilized flames by plotting the ratios of sensitivities according to Eqs. (1)–(3). Local and global similarities of the sensitivity functions of adiabatic methane–air explosions were also demonstrated. Zsély et al. [2] showed that the existence of low-dimensional slow manifolds in chemical kinetic systems might cause local similarity. Scaling relation is present, if the dynamics of the system is controlled by a one-dimensional slow manifold. The rank of the local sensitivity matrix is less than or equal to the dimension of the slow manifold. Global similarity emerges if local similarity is present and the sensitivity differential equations are pseudohomogeneous. Zsély et al. [2] stated that all similarity features could be deduced without using the notion of dominant variable. Moreover, temperature was demonstrated not to be the single dominant variable in the case of the adiabatic explosion of hydrogen–air mixtures, because radical concentrations also have high influence. Zsély and Turányi [9] investigated the relation of the simplification of reaction mechanisms to the similarity of sensitivity functions. They have found that the presence of similarity results in the close coupling of the parameters, but the important parameters were identical in similar models with and without global similarity.

This work is a continuation and extension of the article of Zsély et al. [2]. In all their examples, the combustion of stoichiometric mixtures was investigated. In this work, the scope of the investigation is extended to lean and rich hydrogen–air mixtures. The local similarity of the sensitivity vectors was demonstrated in article [2] by the calculation of the ratio of the sensitivity coefficients according to Eq. (1). If local similarity applies precisely for the system, the resulting curves coincide for all parameters, but this is not a sufficient method if only approximate similarities are present among the sensitivity vectors. New tools for the comparison of sensitivity vectors are introduced here, which can provide new information about chemical kinetic systems and a better understanding of the similarity phenomena of sensitivity vectors.

In Section Sensitivity Analysis of Several Models of Hydrogen–Air Combustion, sensitivity functions are presented for models of hydrogen–air explosions and premixed laminar flames. An appropriate correlation function is introduced in Section Measuring the Similarity of Sensitivity Vectors, which can be used to characterize the relative extent of similarity of sensitivity vectors. In Section Investigation of the Correlation of Sensitivity Vectors by Cobweb Plots, correlation of the sensitivity vectors is investigated by cobweb plots. Correlation of the flame velocity sensitivities with other sensitivity vectors is studied in Section Correlation of the Flame Velocity and Concentration Sensitivities. Conclusions are summarized in the last section.

SENSITIVITY ANALYSIS OF SEVERAL MODELS OF HYDROGEN–AIR COMBUSTION

The Leeds methane oxidation mechanism [10,11] is a modular mechanism that is able to describe the combustion of several simple fuels. In the following calculations, the hydrogen oxidation submechanism was applied that contains nine species (H_2, O_2, H_2O, H_2O_2, H, O, OH, HO_2, and N_2) and 46 irreversible reactions. Irreversibility in this case means that the rates of the forward and backward reaction steps were calculated by separate extended Arrhenius expressions. Arrhenius expressions of the backward reactions were calculated from those of the forward reactions and the thermodynamic data using program MECHMOD [11]. Concentration and temperature profiles, and local sensitivities were calculated by the SENKIN [12] and the PREMIX [13] programs of the CHEMKIN-II package [14]. The cold boundary conditions of the laminar premixed flames were $p = 1$ atm and $T_c = 298.15$ K and the simulations were done at constant pressure. Fuel-to-air ratio φ was 0.5, 1.0, 2.0, and 4.0, corresponding to lean, stoichiometric, moderately rich, and rich compositions, respectively.

Concentration– and temperature–distance functions were calculated for both freely propagating and burner-stabilized adiabatic flames; in the latter simulations the mass flow rate corresponded to that of the equivalent freely propagating flame. The same boundary conditions were used for both types of flames. At the hot boundary, the gradients of concentrations and temperature were zero; therefore, the hot boundary state was equal to the burnt equilibrium state. In the constant pressure, homogeneous explosion calculations, the element composition and the enthalpy of the initial mixture was set to be identical to that of the corresponding laminar flames, therefore the burnt equilibrium states of the explosions and flames were also identical. To

calculate the initial concentrations of homogeneous explosions the following method was used. The hot and the cold boundary compositions of the adiabatic flames were mixed, which resulted in a mixture that had the same element composition and the same enthalpy as those of the initial gas mixtures. The ratio of the cold gas in the mixture was gradually increased, and the composition of the lowest temperature mixture that was able to explode within 10^{-3} s was taken as the initial composition in the homogeneous explosion simulations. Note that this mixture contained radicals in high concentration. The concentration profiles of several major species for all these models in the stoichiometric case can be found in paper [2]. In article [9], the same models were used for the study of the relation of mechanism reduction and similarity of sensitivity functions; a more detailed description of the initial and boundary conditions of these models can be found there.

All calculations were repeated by using a constrained temperature profile. In these cases, the temperature profile was identical to that of the corresponding adiabatic calculations, but was a fixed input of the simulations. Hence, the temperature profile was made independent of the parameter changes. For chemical kinetic reasons, above a certain threshold temperature, the concentration–temperature functions of all hydrogen–air flames and explosions of the same fuel-to-air ratio are very similar, as it has been discussed in article [2].

The local sensitivity functions were also calculated for all systems. In this work, sensitivities of the mass fractions w_i, temperature T, and flame velocity ν_L (the latter in the case of freely propagating flames only) with respect to the preexponential coefficients A_k were analyzed. The sensitivity coefficients were normalized with A_k.

$$s_{ik} = A_k \frac{\mathrm{d}w_i}{\mathrm{d}A_k} = \frac{\mathrm{d}w_i}{\mathrm{d}\ln A_k} \tag{4}$$

In freely propagating flames, the coordinate system is attached to a given temperature point of the flame front (400 K in our simulations), while in burner-stabilized flames the starting point of the coordinate system is the burner surface. It also means that in the former flame, temperature is fixed at one point of the coordinate system. Physically, the freely propagating flames are equivalent to the burner-stabilized flames of equal mass flow rate, therefore the calculated concentration–temperature profiles in these two types of flames agree to the level of numerical accuracy and only the sensitivities are different. It follows that in the case of constrained temperature flame calculations, when the whole temperature–distance profile is fixed, the sensitivity–distance functions of burner-stabilized and freely propagating flames are also identical. Hereinafter sensitivity results for constrained temperature flame calculations will refer to both freely propagating and burner-stabilized flames.

To facilitate the comparison of simulation results for explosions and flames, in all figures the results are plotted as a function of temperature instead of time or distance. Since temperature is a monotone increasing function of time and distance in adiabatic homogeneous explosions and in adiabatic laminar flames, respectively, this is an unambiguous representation of the sensitivity functions.

Figure 1 presents the local sensitivity functions of the mass fractions of OH and H_2O for the adiabatic explosion of hydrogen–air mixtures. The graphs are highly ordered in cases of both species at each hydrogen–air ratio. Since the reactions in the 46-step mechanism are all irreversible, parameter perturbation results in a small displacement of the burnt state. However, the displacement of the equilibrium state is negligible compared to the kinetic effects of parameter perturbations, and the sensitivities are relatively small near the burnt state. At zero time, the sensitivity coefficients for each reaction parameter are zero by definition. There are no a priori expectations on the shape of the sensitivity functions in between. Figure 1 shows that these sensitivity functions are globally similar, that is the ratios of the sensitivity functions remain identical at different temperatures, i.e. $s_{\mathrm{OH},k}(z_1)/s_{\mathrm{OH},m}(z_1) = s_{\mathrm{OH},k}(z_2)/s_{\mathrm{OH},m}(z_2)$, or using a vector equation

$$\mathbf{s}_{\mathrm{OH}}(z_2) = \beta(z_1, z_2)\mathbf{s}_{\mathrm{OH}}(z_1) \tag{5}$$

where z_1 and z_2 are within the region where global similarity is applicable to the system and β is a scalar. It has been mentioned that global similarity can be visualized by plotting the ratio of sensitivities according to Eq. (3). Such plots have been presented in article [2], showing that these functions are globally similar and are not reproduced here.

Also, the relative effect of the change of the individual parameters on the concentrations of OH and H_2O is identical for any z at each fuel-to-air ratio, which can be demonstrated by calculating

$$\lambda_{\mathrm{OH},\mathrm{H_2O},k}(z) = \frac{s_{\mathrm{OH},k}(z)}{s_{\mathrm{H_2O},k}(z)} \tag{6}$$

Figure 2 shows ratio $\lambda_{\mathrm{OH},\mathrm{H_2O},k}$ as a function of temperature for all effective parameters. A parameter is considered effective, if at any value of the independent

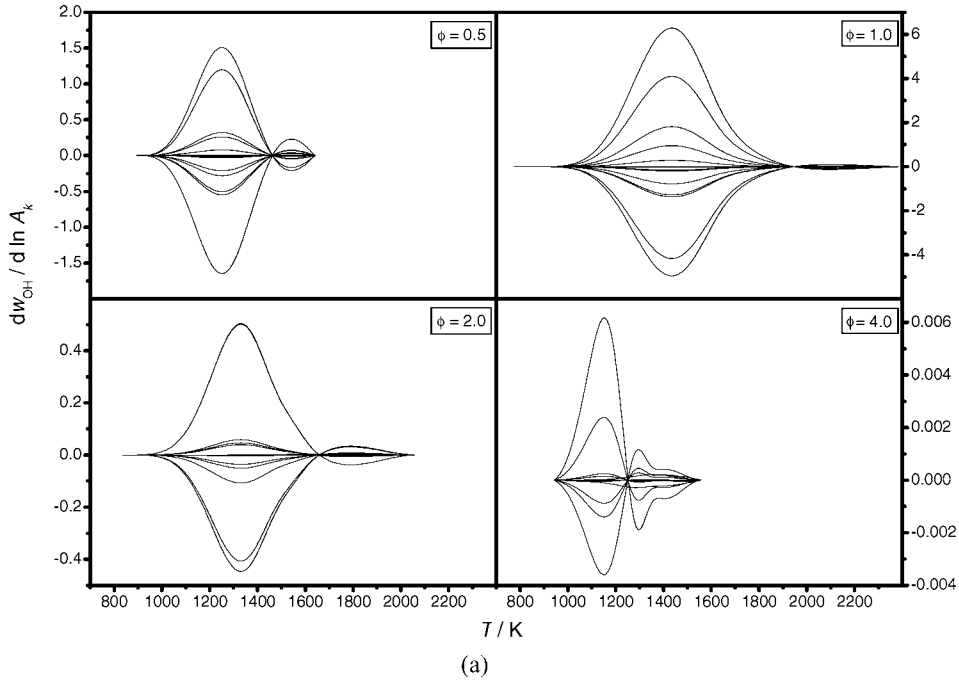

(a)

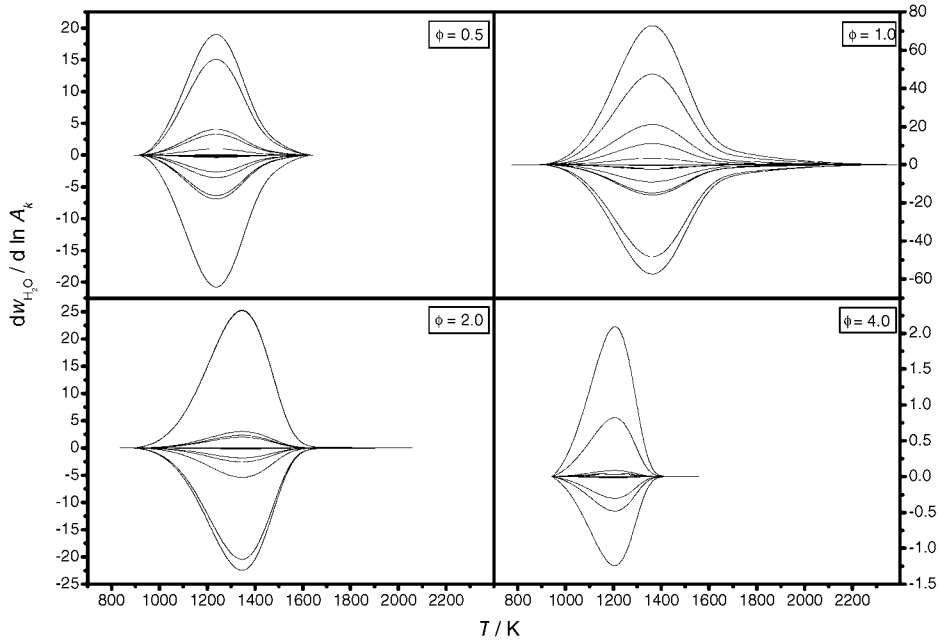

(b)

Figure 1 Sensitivities with respect to the natural logarithm of the 46 preexponential coefficients of the reactions as a function of temperature, calculated for the adiabatic explosion of hydrogen–air mixtures for $\varphi = 0.5, 1.0, 2.0$, and 4.0. Sensitivity coefficients belonging to (a) OH and (b) H_2O are plotted. The sensitivity curves end at the burnt equilibrium temperature. Most of the 46 sensitivity functions are close to zero thus cannot be seen separately.

variable the absolute value of its sensitivity function reaches 5% of the highest absolute sensitivity of the parameter the model output is most sensitive to. The single lines in Fig. 2 demonstrate the exact matching of approximately 15 lines in all cases; deviation occurs only at low and high temperatures. Ratios calculated from the near-zero sensitivity functions do not match to these lines. The most likely reason is that these sensitivity coefficients are calculated with high relative numerical error, because the effect of an ineffective

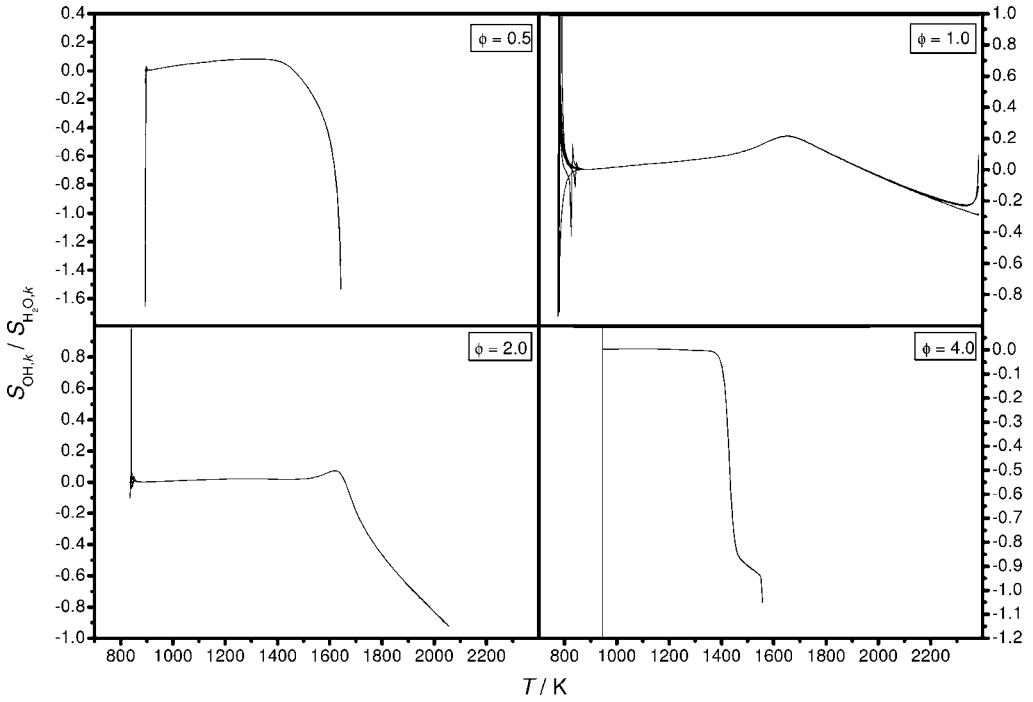

Figure 2 Ratios of the sensitivity functions of OH and H_2O with respect to the same effective parameters ln A_k for the adiabatic explosion of hydrogen–air mixtures. The single lines show the exact matching of the sensitivity ratios.

parameter is comparable to the numerical accuracy of the solver. The property of sensitivity functions that their ratio is equal for any parameter is called [2] *local similarity* [see Eq. (1)]. In most previous papers [4–8], the similarity of sensitivities was demonstrated by plotting the original sensitivity functions only, which is not suitable for the assessment of the level of similarity. Presentations of tables [3] that contain ratios at some selected points contain limited information. A better method is when the appropriate ratios are calculated and plotted (see Fig. 2 and also the figures in article [2]), but this way the similarity of the sensitivity coefficient functions and not of the sensitivity vectors is investigated. Similarity of sensitivity vectors can be quantified by using an appropriate correlation function, which is introduced in the subsequent section.

MEASURING THE SIMILARITY OF SENSITIVITY VECTORS

Existence of local similarity means that any sensitivity vector can be obtained from any other nonzero sensitivity vector, multiplying it by a scalar:

$$\mathbf{s}_i(z) = \lambda_{ij}(z)\mathbf{s}_j(z) \tag{7}$$

where $\mathbf{s}_i(z)$ and $\mathbf{s}_j(z)$ are sensitivity vectors at a given time or distance.

The correlation function ρ, known from mathematical statistics, can be used to investigate the likeness of two vectors [15,16]. It has the form of

$$\rho_{\mathbf{xy}} = \mathrm{cov}_{\mathbf{xy}}/(\sigma_{\mathbf{x}}\sigma_{\mathbf{y}}) \tag{8}$$

where $\mathrm{cov}_{\mathbf{xy}} = \frac{1}{N}\sum_{i=1}^{N}(x_i - \nu_{\mathbf{x}})(y_i - \nu_{\mathbf{y}})$, $\sigma_{\mathbf{x}}^2 = \frac{1}{N}\sum_{i=1}^{N}(x_i - \nu_{\mathbf{x}})^2$, $\sigma_{\mathbf{y}}^2 = \frac{1}{N}\sum_{i=1}^{N}(y_i - \nu_{\mathbf{y}})^2$, and $\nu_{\mathbf{x}}$, $\nu_{\mathbf{y}}$ are the means of the elements of vectors $\mathbf{x} \neq \mathbf{0}$ and $\mathbf{y} \neq \mathbf{0}$, respectively. Although Eq. (8) is usually applied for stochastic variables, it can also be used to characterize the correlation of any two vectors of the same dimension. Correlation analysis determines whether two ranges of data move together. It shows if large values of one vector are associated with large values of the other vector (positive correlation, $\rho = 1$), or small values of one vector are associated with large values of the other vector (negative correlation, $\rho = -1$), or if values in both sets are unrelated (correlation near zero, $\rho = 0$). The correlation values are independent of the magnitude of the vector elements and two vectors are well correlated if all their elements differ in an additive constant. However, this correlation function ρ is not appropriate to investigate local similarity, because two locally similar vectors differ only in a multiplicative constant.

When calculating correlation $\rho_{\mathbf{xy}}$, the vectors $\mathbf{x}$ and $\mathbf{y}$ are shifted by their means, $\nu_{\mathbf{x}}$ and $\nu_{\mathbf{y}}$, respectively. If these shifting terms are left out from Eq. (8) after

simplification we get the following:

$$\tilde{\rho}_{\mathbf{xy}} = \frac{\sum_{i=1}^{N} x_i y_i}{\left(\sum_{i=1}^{N} x_i^2\right)^{1/2}\left(\sum_{i=1}^{N} y_i^2\right)^{1/2}} \tag{9}$$

In Eq. (9) the numerator is the scalar product of the vectors and the denominator is the product of the Eucledian lengths of the vectors. Hence, we can write Eq. (9) in the following form:

$$\tilde{\rho}_{\mathbf{xy}} = \frac{\mathbf{xy}}{\|\mathbf{x}\|\|\mathbf{y}\|} \tag{10}$$

where $\|\mathbf{x}\|$ and $\|\mathbf{y}\|$ are the Eucledian lengths of the vectors. Moreover, it is recognized [15,16] that

$$\tilde{\rho}_{\mathbf{xy}} = \cos\theta_{\mathbf{xy}} \tag{11}$$

where $\theta_{\mathbf{xy}}$ is the angle of the two vectors and it is clear that $-1 \leq \tilde{\rho} \leq +1$, similarly to correlation function ρ.

It is apparent that correlation function $\tilde{\rho}$ is a good measure of the local similarity of sensitivity vectors. According to Eq. (7), two sensitivity vectors are locally similar if the ratio of their vector components is the same, i.e. they point to exactly identical or opposite direction in the N-dimensional space of the parameters. This means that their angle is either 0 or 180°, which is equivalent to a $\tilde{\rho}_{ij} = \pm 1$. Correlation $\tilde{\rho}_{ij} = +1$ means that the sensitivity vectors are locally similar and there is a positive correlation between the elements; perturbing the values of the parameters changes the calculated values of variables i and j into the same direction. If $\tilde{\rho}_{ij} = -1$, then the sensitivity vectors are also locally similar, but there is negative correlation between them, and perturbing the values of the parameters changes the values of variables i and j into opposite directions. If $\tilde{\rho}_{ij}$ is not close to ± 1, then the sensitivity vectors are poorly correlated and are not locally similar.

All sensitivity vectors of the hydrogen–air combustion, that is sensitivities calculated for homogeneous explosions, freely propagating and burner-stabilized flames at adiabatic and constrained temperature conditions were investigated by plotting the $\tilde{\rho}_{ij}(z)$ functions and this analysis was carried out at all fuel-to-air ratios ($\varphi = 0.5$, 1.0, 2.0, and 4.0). The plots are produced so that $\tilde{\rho}_{ij}(z)$ functions of all sensitivity vectors i were calculated with respect to a selected reference sensitivity vector j from the same dataset. Several reference sensitivity vectors were tried; in all cases to be discussed here the reference vector was the water concentration sensitivity vector. It was chosen because it is an appropriate reaction progress indicator and its concentration is monotone increasing function of temperature.

The plots (see Figs. 3–6) obtained show characteristic changes of correlations and most of these functions could be interpreted using chemical kinetic reasoning. Because of the stoichiometry of the overall reaction and because the concentrations of H_2, O_2, and H_2O are much larger than those of the other species, the

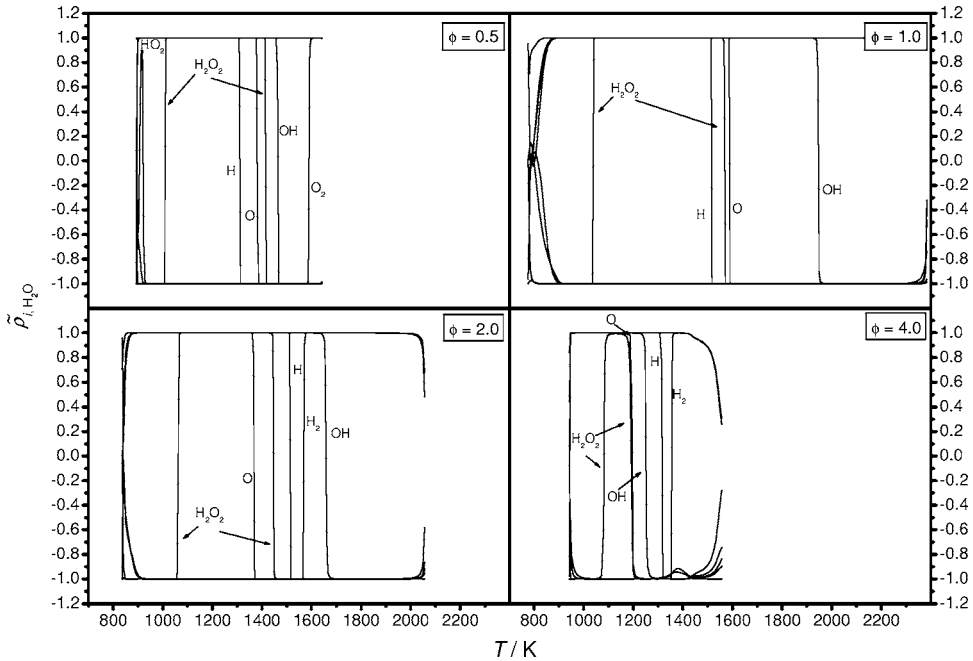

Figure 3 Correlation as a function of temperature, comparing the sensitivity vector of water concentration to the sensitivity vectors of the concentrations of the other species in the case of homogeneous adiabatic explosion of hydrogen–air mixtures.

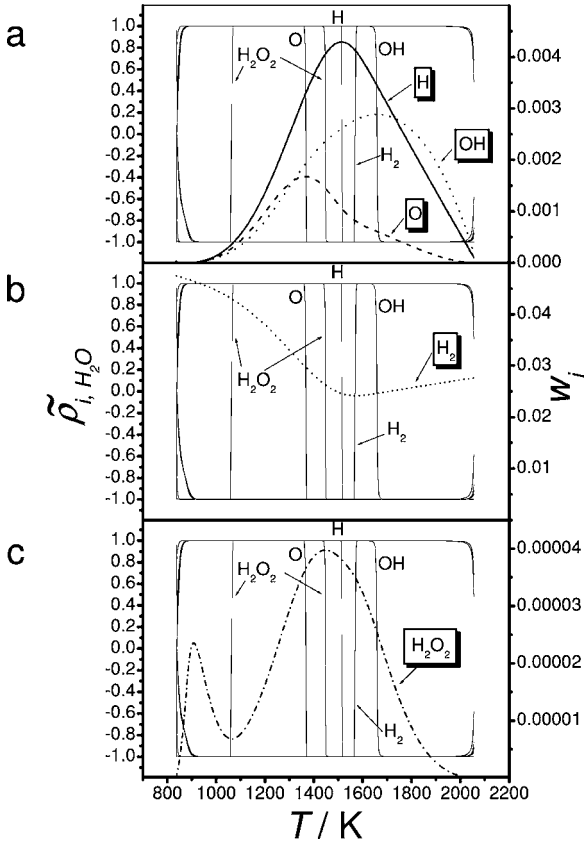

Figure 4 Correlation function (left axis) and concentration profiles (right axis) for the case of $\varphi = 2.0$ adiabatic explosion. Concentration curves are denoted by (a) straight line: H, dotted line: OH, dashed line: O, (b) short dashed line: H_2 and (c) dash-dotted line: H_2O_2.

sensitivity vectors of H_2 and O_2 are always negatively correlated with the sensitivity vector of water in stoichiometric flames and explosions. In rich mixtures, there is a significant formation of H_2 from radicals after the flame front (or explosion), therefore hydrogen molecule sensitivities become positively correlated with that of water. The same happens with the oxygen molecule sensitivities in lean mixtures. Since most of the heat release comes from the reactions of water formation, the temperature sensitivity vector is always positively correlated with the water sensitivity vector. There are no general tendencies for the correlation functions of other species and these have to be interpreted separately in each case.

Figure 3 shows the $\tilde{\rho}_{i,\mathrm{H_2O}}$ values as a function of temperature for the adiabatic explosion of hydrogen–air mixtures for $\varphi = 0.5$–4.0, where i = T, H, O_2, H_2O_2, H, O, OH, HO_2, N_2. In general, the sensitivity vectors are very similar to each other, but at certain points the direction of the correlation sharply changes from -1 to $+1$ or vice versa. These points coincide with the location of the local minimum or maximum of the concentrations of the corresponding species, i.e., where their derivative with respect to time is zero. Increasing the fuel-to-air ratio, the level of similarity is lower and the range of the transition temperature gets slightly wider.

In the case of adiabatic hydrogen–air explosions, the ratio $\lambda_{ij}(z)$ was found [2] to be identical to the ratio of the corresponding production rates, therefore

$$\mathbf{s}_i(z) = \frac{\frac{\mathrm{d}Y_i}{\mathrm{d}t}(z)}{\frac{\mathrm{d}Y_j}{\mathrm{d}t}(z)}\mathbf{s}_j(z) \tag{12}$$

This observation means the existence of the *scaling relation* [see Eq. (2)].

According to Eq. (12), a positive ratio of production rates results in a positive scaling factor λ_{ij} between the vector components and a negative ratio results in a negative λ_{ij}. Also, Eq. (12) predicts zero sensitivity coefficients of variable i at the point(s) of local extreme of the same variable. Sensitivity vector $\mathbf{s}_j$ is the sensitivity of water concentration in our case, which assures that the denominator is never zero, since water concentration is a monotonic function of time in the case of all systems investigated here. Moreover, the denominator is always positive, because the water concentration is monotone increasing. This means that the location of the correlation changes reflect the properties of the sensitivity vectors of variables i and not that of the water sensitivity. The correlation changes are labelled in the graph with the name of the corresponding species. In reality, however, coefficients of sensitivity vector $\mathbf{s}_i$ are small but not zero at these points. This can be expressed by supplementing the original scaling relation [Eq. (12)] with a correction vector $\mathbf{s}'_j$:

$$\mathbf{s}_i(z) = \frac{\frac{\mathrm{d}Y_i}{\mathrm{d}z}(z)}{\frac{\mathrm{d}Y_j}{\mathrm{d}z}(z)}\mathbf{s}_j(z) + \mathbf{s}'_j(z) \tag{13}$$

where $\|\mathbf{s}_j(z)\| \gg \|\mathbf{s}'_j(z)\|$ and there is no correlation between sensitivity vectors $\mathbf{s}_i$ and $\mathbf{s}'_j$. If the ratio of the gradients is large, then $\mathbf{s}_i(z) \approx \lambda_{ij}\mathbf{s}_j(z)$ and $\tilde{\rho}_{ij} \approx \pm 1$. However, if the ratio is small (at the extremes of the value of variable Y_i), then the sensitivity vectors are not similar and it results in an intermediate $\tilde{\rho}_{ij}$ value.

If scaling relation (12) is valid, then the changes in correlation coincide with the local concentration extreme of the appropriate species. Figure 4 shows that for adiabatic explosions of hydrogen–air mixtures at $\varphi = 2$, the locations where $\tilde{\rho}_{i,\mathrm{H_2O}} = 0$ at the change of correlation and the concentration extremes coincide. The same coincidence, within the numerical precision of the simulations, from about 950 K to near the burnt equilibrium temperature was justified in the cases of all

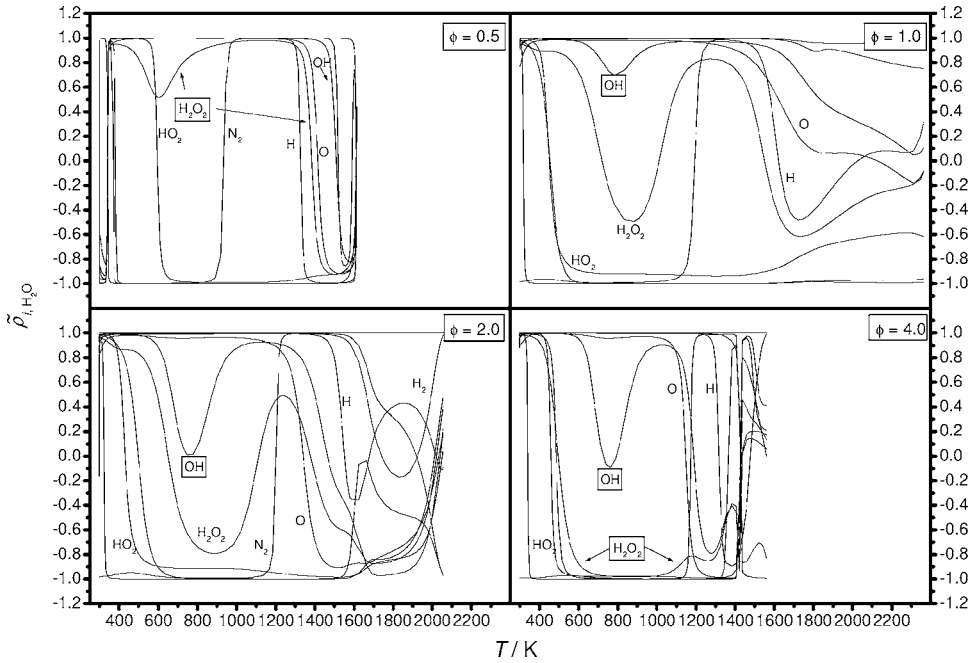

Figure 5 Correlation as a function of temperature, comparing the sensitivity vector of water concentration to the sensitivity vectors of the concentrations of the other species in the case of adiabatic burner-stabilized flames. Scaling relation is valid for all correlation changes except for when the name of the corresponding species is boxed.

fuel-to-air ratios investigated for adiabatic hydrogen–air explosions.

In the low temperature region the kinetic processes are very slow and in the high temperature region the features of the system are controlled by the thermodynamics rather than the kinetics and this is the reason for the lack of local similarity and scaling relation in these regions.

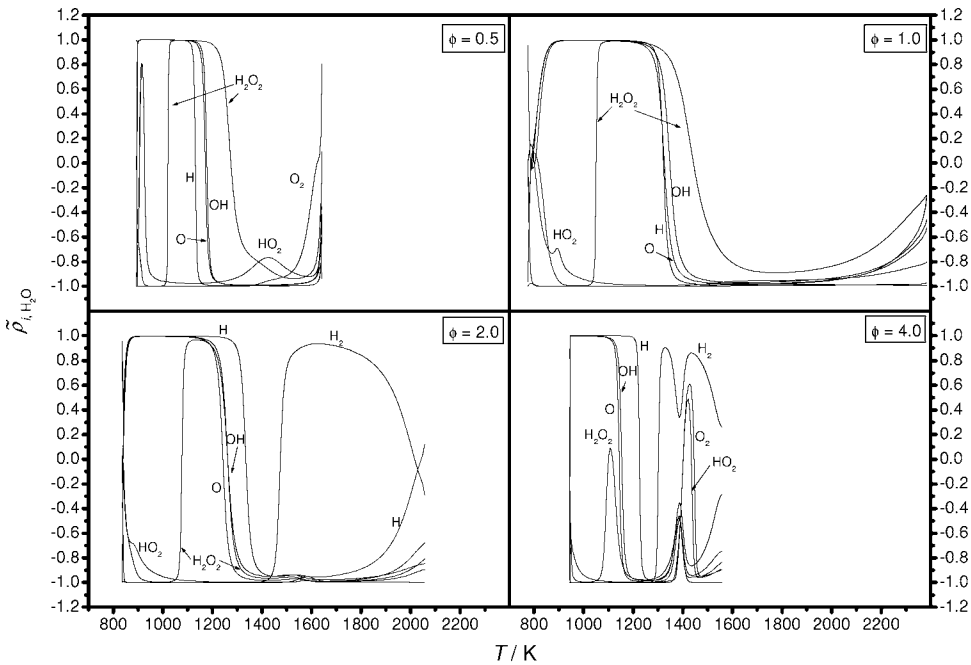

Figure 6 Correlation as a function of temperature, comparing the sensitivity vector of water concentration to the sensitivity vectors of the concentrations of the other species in the case of constrained temperature explosions.

Figure 5 presents function $\tilde{\rho}_{i,H_2O}$ for adiabatic burner-stabilized hydrogen–air flames. The similarity is much poorer than for adiabatic explosions. Zero correlations ($\tilde{\rho}_{i,H_2O} = 0$) coincide with the extremes of the concentration functions, although not as precisely as in the case of adiabatic explosions. This difference can be attributed to the presence of diffusion [2]. In cases of some species, in a temperature range the correlation is poor with the water sensitivity vector, i.e., the absolute value of the correlation function is lower than about 0.6. However, these regions are not related to the concentration extremes of these species. Correlation functions of such property are marked with black boxes in Fig. 5, and these belong to species H_2O_2 and OH. The zones of correlation change are wider compared to those of the adiabatic explosions of identical element composition mixtures, but the width does not increase with increasing fuel-to-air ratio. Note, that the correlation of N_2 sensitivities with water sensitivities also changes, and these changes also correspond to the concentration extremes of N_2. Nitrogen is not a reactive gas in the mechanism, but the concentration of N_2 has a definite maximum in the flame front, because pressure is kept constant and all intermediates diffuse outwards from the flame front. Therefore, in flames the mass fraction of N_2 may change slightly as a result of parameter perturbation.

In the cases of constrained temperature explosions, the correlations of the sensitivities also change sharply, but these changes cannot be assigned to the concentration extremes and the overall similarity is somewhat poorer. Figure 6 shows that in the cases of constrained temperature explosions, the correlation functions of each species follow a pattern similar to the adiabatic explosion cases. On the other hand, the changes of correlations are elongated and occur at different temperatures than in the adiabatic case. Good correlation of the sensitivity vectors in some regions is in accordance with the manifold explanation [2] of the local similarity of sensitivities, since low-dimensional slow manifolds exist also in constrained temperature kinetic systems. The assumption [3] that the cause of similarity of sensitivity vectors is the calculated temperature as a single dominant variable predicts no correlation of sensitivity vectors for constrained temperature explosions.

In the rest of the cases (freely propagating adiabatic flames and constrained temperature flames), the overall level of similarity is much lower and the correlation changes do not coincide with the concentration extremes. Only the sensitivity vectors of H_2 and O_2 are well correlated with that of the water concentration, similarly to the other cases. The correlation functions of all other species mainly run in the range $+0.6$ to -0.6, that is no good correlation was found.

The advantage of function (10) is that it quantifies the local similarity of two sensitivity vectors with a single number and the change of the similarity relation can be examined as a function of the independent variable or temperature. On the other hand, a reference vector has to be selected for the comparison. Also, it does not provide information about the details of the correlation of the vectors.

INVESTIGATION OF THE CORRELATION OF SENSITIVITY VECTORS BY COBWEB PLOTS

Anatomy of the changes of the correlations can be investigated by *cobweb plots*. Cobweb plots are suitable tools [17] for the study of the correlation of several vectors simultaneously. Cobweb plots have the advantage that no distinguished vector should be selected, which allows a nonbiased identification of correlations. In the cobweb plots used in this paper, each vertical section represents a sensitivity vector in such a way that the highest positive vector element belongs to the top, zero vector elements belong to the middle, and the lowest negative element belongs to the bottom of the section. All other positive and negative vector elements are linearly scaled between the top and the middle as well as the middle and the bottom points, respectively. A point that corresponds to parameter k of a sensitivity vector on a section is connected to the point of the same parameter k on the neighbouring sections. Parallel lines on a cobweb plot mean positive correlation between the two neighbouring sensitivity vectors, an asterisk shape is the sign of negative correlation, while nonorderly patterns indicate noncorrelated sensitivity vectors.

Figure 7 shows the correlation of sensitivity vectors of the adiabatic stoichiometric hydrogen–air explosion near the point where OH has a maximum in concentration and also where its correlation with water changes (see Fig. 3). Preceding the concentration maximum of OH, the sensitivity vectors of H_2, O_2, HO_2, H, O, and H_2O_2 are positively correlated with each other; another positively correlated group is the sensitivities of OH, H_2O, and temperature. The two groups are negatively correlated with each other. This means that all parameter changes that decrease the concentrations of OH, H_2O, and temperature, increase the concentration of all other species. Cobweb plots show that where the OH concentration is maximal, its sensitivity is not correlated with any other sensitivity vector, but after the maximum it becomes positively correlated with the sensitivities of all variables but temperature and the concentration of water. In all other cases of homogeneous adiabatic explosions the correlation changes can

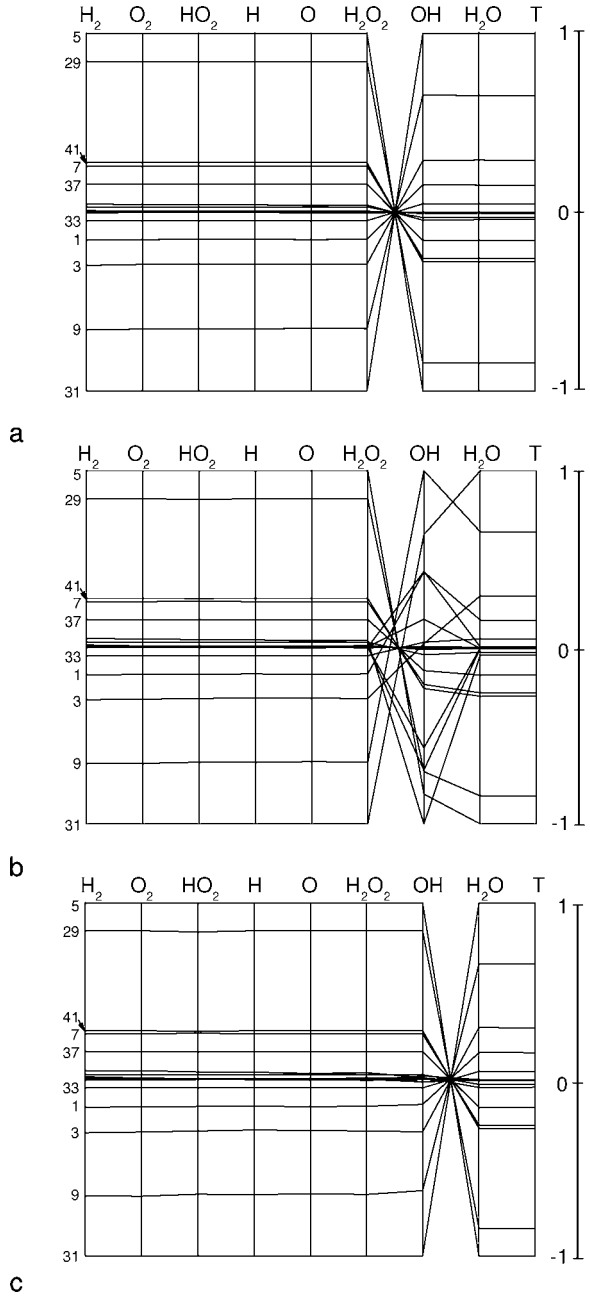

Figure 7 Anatomy of the correlation change belonging to radical OH in Fig. 3 at $\varphi = 1.0$. Cobweb plots of the sensitivity vectors are shown (a) before (1740 K), (b) at (1945 K), and (c) after (2040 K) the correlation change. At 1740 K the sensitivity vector of radical OH is positively correlated with product H_2O, but becomes negatively correlated with it after the correlation change. There is a lack of correlation in between. Numbers on the left-hand side indicate reactions, which can be found in Table I.

be traced back in a similar way to the change of correlation of the corresponding sensitivity vectors.

Correlation changes indicate the crossover between two kinetic regimes, because the sensitivity functions of a given species change sign at these points. Let us consider the case of OH (see Figs. 3 and 7; for the corresponding list of reactions see Table I). Reactions 31, 9, 3, 1, and 33 are mainly chain branching reactions. Reactions 5, 29, 41, 7, and 37 are chain-terminating reactions or produce less reactive HO_2 from the reactive radical H. Between 1600 K and about 1945 K, increasing the rate coefficients of the reactions in first group decrease of the concentrations of the reactants H_2 and O_2, and therefore decrease the concentrations of all radicals but OH. Above about 1945 K, the concentration of OH is also decreased. Increasing the rate coefficients of the reactions in the second group has always an opposite effect.

It is often assumed that the kinetic regimes are separated by the minimum or maximum of the species concentrations. Investigation of the correlation changes offers an alternative way for the selection of the kinetic regimes, which is in better agreement with the actual kinetic processes. In the cases of some systems, where the scaling relation is valid, this recommended procedure coincides with the previous practice.

CORRELATION OF THE FLAME VELOCITY AND CONCENTRATION SENSITIVITIES

Laminar flame velocity ν_L is a physical constant of freely propagating flames that depends only on the composition, the temperature, and the pressure of the initial gas mixture [18]. Comparison of experimentally measured and calculated flame velocities

Table I Reactions of High Sensitivity at Stoichiometric Hydrogen–Air Explosions and Flames (See Figs. 7 and 10)

No.	Reaction
1	$H_2 + O \rightarrow OH + H$
2	$OH + H \rightarrow H_2 + O$
3	$H_2O + H \rightarrow H_2 + OH$
4	$H_2 + OH \rightarrow H_2O + H$
5	$O_2 + H + M \rightarrow HO_2 + M$
7	$O_2 + H + H_2O \rightarrow HO_2 + H_2O$
9	$O_2 + H \rightarrow OH + O$
10	$OH + O \rightarrow O_2 + H$
20	$H_2O_2(+M) \rightarrow 2OH(+M)$
21	$2H + M \rightarrow H_2 + M$
25	$H + O + M \rightarrow OH + M$
27	$H + OH + M \rightarrow H_2O + M$
29	$H + HO_2 \rightarrow H_2 + O_2$
31	$H + HO_2 \rightarrow 2OH$
33	$H + HO_2 \rightarrow H_2O + O$
37	$O + HO_2 \rightarrow O_2 + OH$
41	$OH + HO_2 \rightarrow H_2O + O_2$

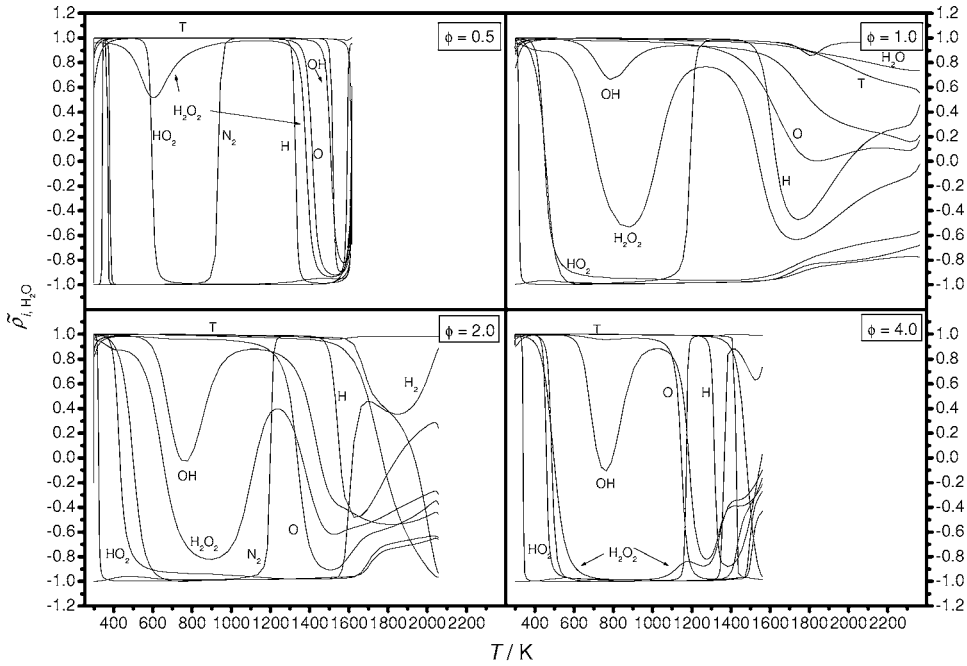

Figure 8 Correlation as a function of temperature, comparing the flame velocity sensitivity vector to the sensitivity vectors of the concentrations and temperature in the cases of adiabatic burner stabilized flames.

in a wide range of fuel-to-air ratio is an extensively used method for testing combustion mechanisms (see e.g. [10]). Presentation of new or modified combustion mechanisms is frequently accompanied with the investigation of the sensitivity of flame velocity to parameter perturbations. There is a common assumption that the ranking of flame velocity sensitivities provides a general rank order of the importance of reactions in combustion mechanisms. To check this assumption, correlation of the sensitivity vector of flame velocity with that of species concentrations was investigated.

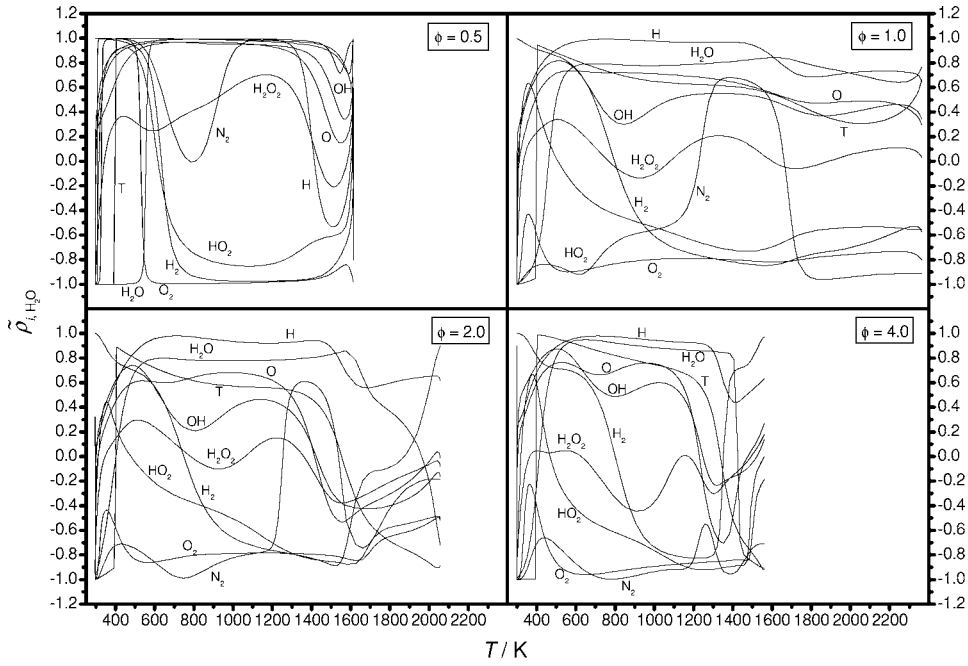

Figure 9 Correlation as a function of temperature, comparing the flame velocity sensitivity vector to the sensitivity vectors of the concentrations and temperature in the cases of freely propagating adiabatic flames.

The correlation functions of the sensitivity vectors of each species with the flame velocity sensitivity vector in the cases of adiabatic burner-stabilized flames were investigated (see Fig. 8). In the case of a stoichiometric mixture, the sensitivity vectors of temperature and the concentration of each species are well correlated (positively or negatively) with the sensitivity vector of flame velocity in the temperature range 1200–1500 K, that is in the region of the flame front. It could be expected that the kinetic information of the flame velocity sensitivities correspond to the kinetic processes in the flame front. The temperature region of the flame front slightly changes with φ and at each fuel-to-air ratio in the corresponding temperature region the flame velocity sensitivity vector shows good correlation with the sensitivity vectors of most species.

In the cases of adiabatic freely propagating flames (see Fig. 9), the sensitivity vectors of most species do not have a good correlation with the flame velocity sensitivity vector for any temperature region and fuel-to-air ratio. The correlation is somewhat better for leaner mixtures and in the flame front region of each flame. The reason of the great difference between the sensitivity functions of burner-stabilized and freely propagating flames is that in the former flames the flame front may move significantly due to parameter perturbation and then most species concentrations change in a concerted way, while in the latter flames the location of the flame in the coordinate system of the calculations is fixed (at $T = 400$ K) and the sensitivities reflect only the relative change of species concentrations.

The hydrogen atom and water have distinguished kinetic role in the hydrogen–air combustion system. The H-atom is one of the main chain carriers in the chain reaction and the diffusion of it is crucial in flame propagation. It can be expected that any parametric change that increases the H-atom concentration in the flame front region also increases the flame speed. Water is the single product of the combustion reaction and increased flame speed is linked with enhanced water production. The flame velocity sensitivities have good positive correlation at all fuel-to-air ratios with the sensitivity vectors of these two species in the front region of adiabatic flames. Part (a) of Fig. 10 is a cobweb plot showing that at 1400 K and $\varphi = 1.0$, the flame velocity sensitivity vector has good correlation with the water concentration sensitivity vector in the case of adiabatic burner-stabilized flames. The correlation is worse in the cases of adiabatic freely propagating and constrained temperature flames, and very bad for homogeneous explosions. Part (b) of Fig. 10 shows that the sensitivity vector of ν_L has good correlation with the H-atom concentration sensitivity vector of adiabatic burner-stabilized and freely propagating flames, and less good with that of constrained temperature flames. The H-atom sensitivity vectors of adiabatic and constrained temperature explosions negatively correlate with each other, but the correlation is poor with the sensitivity vector of flame velocity. The conclusion is that the rank of reactions based on the flame velocity sensitivities well depict the importance of reactions for the H-atom concentration in the front of adiabatic flames, but it cannot be used to characterize the importance of the reaction steps in a combustion system in general.

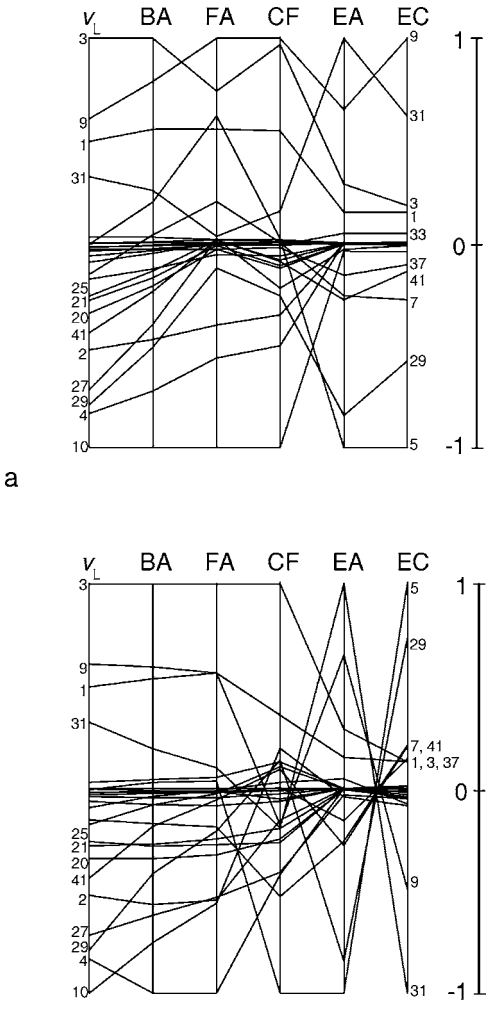

Figure 10 Cobweb plots for the comparison of the flame velocity sensitivity vector (ν_L) with the sensitivity vectors of (a) H_2O and (b) H at the following conditions: adiabatic burner-stabilized flame (BA), adiabatic freely propagating flame (FA), constrained temperature flames (CF), adiabatic explosion (EA), and constrained temperature explosion (EC). All sensitivities are calculated for stoichiometric hydrogen–air combustion and the concentration sensitivities belong to $T = 1400$ K. Numbers on the left-hand side refer to reactions, which can be found in Table I.

CONCLUSIONS

If the variables of a dynamical model are strongly coupled, the values of all variables change in a concerted way when a parameter is perturbed. This feature of dynamical systems is manifested in the *similarity relations* among the sensitivity coefficients. Local similarity, scaling relation, and global similarity were detected in several chemical kinetic models. The local similarity of sensitivity vectors means that any sensitivity vector can be obtained from any other nonzero sensitivity vector by multiplying it by a scalar: $\mathbf{s}_i(z) = \lambda_{ij}(z)\mathbf{s}_j(z)$. Previously, local similarity was identified by calculating and comparing the elements of sensitivity vectors [2,3], but this method is not applicable when only approximate local similarity is present.

This paper presents a thorough investigation of the local sensitivity concept. If the calculated values of two variables in a model respond similarly to the perturbation of all parameters, this means that the corresponding two parameter vectors are locally similar. Such behaviour always has some physical background, that is why the investigation of local similarity may contribute to the exploration of the physical basis of chemical kinetic models. Moreover, the presence of local similarity has significant consequences on parameter estimation procedures if all data points are located in a narrow region of time or distance, as it has been described in more details in articles [2] and [9]. In case of models having global similarity, if physical parameters are deduced by fitting to experimental data, errors in the fixed parameters result in that the determined values will be wrong even if the agreement between the data and the calculated values is excellent for all measured variables. Local similarity is a prerequisite of global similarity [2], therefore the investigation and quantification of local similarity is crucial.

In this paper, two methods are used to study the local similarity of sensitivity vectors. The $\tilde{\rho}_{ij}(z)$ correlation function (10) characterizes the local similarity of two sensitivity vectors with a single number. It can be used to reveal the local similarity of the sensitivity vectors of the species with a reference sensitivity vector in the whole range of the independent variable. A disadvantage of this function is that a reference vector should be selected, preferably a sensitivity vector with monotonous properties. The other disadvantage is that details of the correlation remain hidden. Perfect local similarity results in $\tilde{\rho}_{ij}(z) = \pm 1$ and at the regions of poor similarity typically $-0.6 < \tilde{\rho}_{ij}(z) < +0.6$.

Cobweb plots are suitable tools for the simultaneous study of the correlation of several vectors. In this case, no distinguished vector should be selected, the correlation patterns are striking and the influence of individual parameters can be traced. This approach has the drawbacks that it gives only a qualitative characterization of the level of correlation and also that each cobweb plot belongs to a single value of the independent variable.

This paper focuses on the investigation of local similarity and scaling relation. Note, that the methods above could be used also for the study of global similarity, because in that case also vectors should be compared [see Eq. (5)].

Combustion of hydrogen is a frequently investigated chemical system concerning the similarity of sensitivity vectors [2,3,5,7]. In these articles mainly the combustion of stoichiometric hydrogen–air mixtures were investigated and usually only at some special conditions. In this paper, the correlation of sensitivity vectors was investigated at all the 24 combinations of the conditions below:

- homogeneous explosions, freely propagating, or burner-stabilized laminar flames,
- adiabatic conditions or using a temperature profile fixed to the adiabatic temperature curve,
- fuel-to-air ratios 0.5, 1.0, 2.0, and 4.0.

At a given fuel-to-air ratio, the initial and boundary conditions were selected to provide similar concentration–temperature curves in each case.

Investigation of the various hydrogen–air combustion systems revealed that local similarity and scaling relation is valid for the homogeneous adiabatic explosions with high precision at most times. Using the water sensitivity vector for comparison, the correlation function changed from -1 to 1 or from 1 to -1 in a very narrow temperature range at the concentration extremes of the corresponding species. Cobweb plots showed that the changes of correlation corresponded to the rearrangement of the groups of variables having similar correlation. In the cases of adiabatic burner-stabilized flames and constrained temperature explosions, the overall level of similarity was lower, and the change of the sign of correlation was elongated. No correlations were found in the cases of freely propagating flames and constrained temperature burner-stabilized flames, except for the correlations among the sensitivity vectors of w_{H_2}, w_{O_2}, w_{H_2O}, and T.

In the recent article of Zsély et al. [2], a theoretical explanation was given for the local similarity, scaling relation, and global similarity of sensitivity functions of chemical kinetic models. According to their description, existence of low-dimensional slow manifolds in spatially homogeneous chemical kinetic systems may cause local similarity, and scaling relation is present

if the slow manifold is one-dimensional. In reaction–diffusion systems, like in laminar flames, the similarity relations are weakened due to the presence of diffusion. In the present paper, a more in-depth investigation of hydrogen–air combustion systems was carried out and all results were in good agreement with the predictions of Zsély et al. [2].

Correlation functions and cobweb plots are well applicable to study the relation of the sensitivity vector of flame velocity to the sensitivity vectors of species concentrations. In the case of burner-stabilized flames, effective parameter perturbations change the calculated distance of the flame front from the burner surface. Consequently, all concentrations change in a concerted way and the flame velocity sensitivity vector has good correlation with the sensitivity vectors of most species in the flame front. In the case of freely propagating flames, the coordinate system is attached to the flame sheet and therefore the flame velocity sensitivity vector has good correlation only with the sensitivity vectors of H and H_2O concentrations in the flame front, which can be explained by the special role of these species in hydrogen–air flames. No correlation of the flame velocity sensitivities with the H and H_2O concentration sensitivities of explosions was found, which means that the flame velocity sensitivities are not applicable generally for the characterization of combustion systems.

The authors acknowledge the helpful discussions with K. Héberger, T. Nagy, A. S. Tomlin, and J. Tóth.

BIBLIOGRAPHY

1. Tomlin, A. S.; Turányi, T.; Pilling, M. J. In Low-Temperature Combustion and Autoignition; Pilling, M. J.; Hancock, G. (Eds.); Elsevier: Amsterdam, 1997; pp. 293–437.
2. Zsély, I. Gy.; Zádor, J.; Turányi, T. J Phys Chem A 2003, 107, 2216–2238.
3. Rabitz, H.; Smooke, M. D. J Phys Chem 1988, 92, 1110–1119.
4. Reuven, Y.; Smooke, M. D.; Rabitz, H. J Comput Phys 1986, 64, 27–55.
5. Smooke, M. D.; Rabitz, H.; Reuven, Y.; Dryer, F. L. Combust Sci Technol 1988, 59, 295–319.
6. Mishra, M. K.; Yetter, R. A.; Reuven, Y.; Rabitz, H. Int J Chem Kinet 1994, 26, 437–453.
7. Vajda, S.; Rabitz, H.; Yetter, R. A. Combust Flame 1990, 82, 270–297.
8. Vajda, S.; Rabitz, H. Chem Eng Sci 1992, 47, 1063–1078.
9. Zsély, I. Gy.; Turányi, T. Phys Chem, Chem Phys 2003, 5, 3622–3631.
10. Hughes, K. J.; Turányi, T.; Clague, A. R.; Pilling, M. J. Int J Chem Kinet 2001, 33, 513–538.
11. Combustion simulations at the Leeds University and at the ELTE, http://www.chem.leeds.ac.uk/Combustion/Combustion.html, http://garfield.chem.elte.hu/Combustion/Combustion.html.
12. Lutz, A. E.; Kee, R. J.; Miller, J. A. Sandia National Laboratories, Report No. SAND87-8248, 1987.
13. Kee, R. J.; Grcar, J. F.; Smooke, M. D.; Miller, J. A. Sandia National Laboratories, Report No. SAND85-8240, 1985.
14. Kee, R. J.; Rupley, F. M.; Miller, J. A. Sandia National Laboratories, Report No. SAND89-8009B, 1989.
15. Saville, D. J.; Wood, G. R. Statistical Methods: A Geometric Approach; Springer-Verlag: New York, 1991.
16. Dean, E. B. Proceedings of the Fifteenth Annual Conference of the International Society of Parametric Analysts, San Francisco, CA, 1993.
17. Cooke, R. M.; van Noortwijk, J. M. In Sensitivity Analysis; Saltelli, A.; Scott, E. M.; Chen, K. (Eds.); Wiley: Chichester, 2000; pp. 245–264.
18. Glassmann, I. Combustion, 3rd ed.; Academic: San Diego, 1996.